

Design and Simulations of the Trigger Electronics for the CMS Muon Barrel Chambers

M. De Giorgi, F. Gasparini, I. Lippi, R. Martinelli, P. Zotto and G. Zumerle
I.N.F.N. Padova, Italy

1 - INTRODUCTION

The baseline solution for the barrel muon detector of the CMS [1] experiment consists of self-triggering arrays of drift tubes called DTBX (Drift Tubes with Bunch Crossing identification).

The performance of the mean-timer trigger technique applied to arrays of drift tubes was studied [2] in the RD5 [3] setup. The mean-timer allows the association to a bunch crossing (bx) of a track starting from the signals collected on the wires of at least three layers of staggered drift tubes.

A robust and efficient mean-timer technique, insensitive to wire inefficiencies and able to get a fast measurement of the track impact parameters, needs to be developed. Robustness requires a minimum number of four planes of drift tubes; in this way an inefficiency or a δ -ray spoiling the drift time measurement in one tube leaves anyway three useful cells, giving the minimum quantity of information necessary for the bunch crossing identification. Infact if the drift time of a tube is missing or wrong due to the presence of a δ -ray, the crossing time is still identifiable by a device looking for all the possible three out of four hits alignments.

If the discriminated wire signals are shifted, in the same direction of their drift at bunch crossing frequency in a register of depth equal to the maximum drift time T_{MAX} , the hits will be aligned in the shift registers after an interval T_{MAX} from the track crossing time as shown in Fig. 1.

The time of alignment in the registers identifies the bunch crossing time and gives a measurement of the track impact parameters with a resolution related to the shift frequency: the aligned points are images of the track hits and then the track impact position and the track direction can be calculated from the shift times t_s .

The DTBX chamber cross section in the bending plane of CMS is shown in Fig. 2.

The chamber consists of twelve layers of drift tubes arranged in three Super Layers (SLs) of four planes each: the two outer SLs measure the coordinate in the bending plane (ϕ view) and the intermediate SL the longitudinal coordinate along the beam line (θ view). A 10 cm thick aluminium honeycomb is sandwiched between the planes to increase the chamber stiffness and the lever arm between the ϕ view measurements.

For a nominal drift velocity $V_d = 50\mu\text{m/ns}$ we have

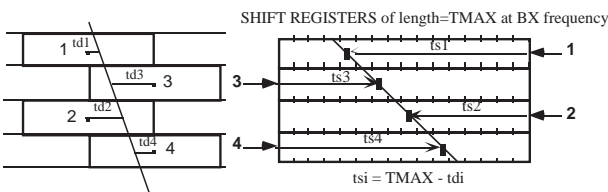


Fig. 1: Mean Timer alignment technique.

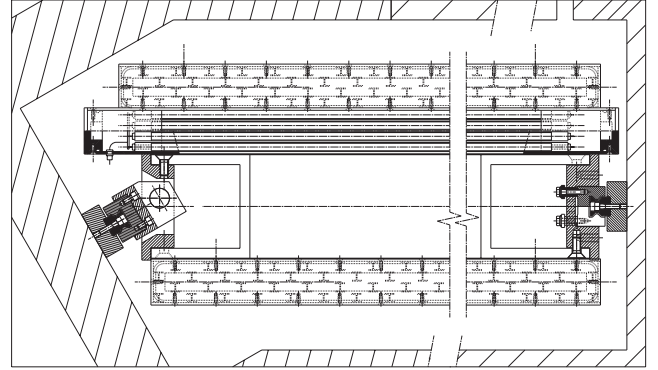


Fig. 2: DTBX chamber cross section in the bending plane.

therefore $T_{MAX} = 400\text{ns}$ (corresponding to 16bx).

2 - TRIGGER ELECTRONICS OVERVIEW

The block diagram of the chamber trigger is shown in Fig. 3.

The trigger front-end device, called Bunch and Track Identifier (BTI), is used in both chamber views to measure position and direction of trigger candidate tracks giving at least three hits, in different planes of a SL, aligned within a programmable angular acceptance. In the θ view only tracks pointing to the vertex are selected.

In the bending plane a Track Correlator (TC) is used to filter the information of the two SLs of a chamber in order to lower the trigger noise and to select, at every cycle among the trigger candidates, the two tracks with the smallest angular distances with respect to the radial direction to the vertex.

TC trigger data are transmitted to the chamber Trigger

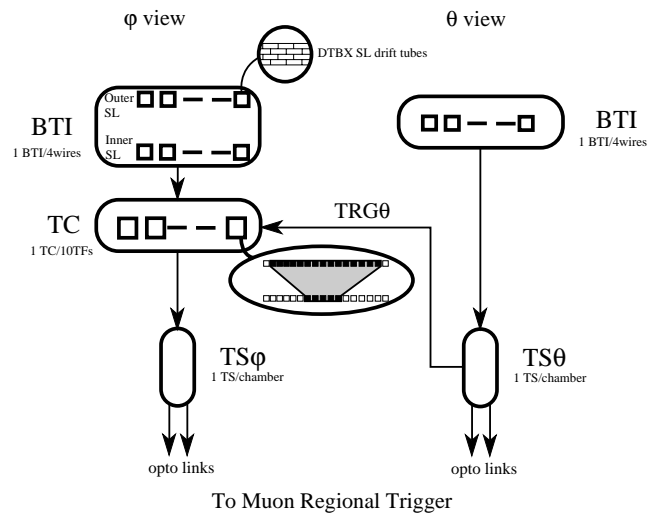


Fig. 3: Block scheme of DTBX chamber trigger electronics.

Server (TS): the TS of the ϕ view (TS ϕ) selects again two tracks (looking for the lowest ϕ bending) among all tracks transmitted by the TCs; the TS of the θ view (TS θ) sends the wired-or of the BTI trigger outputs to TCs and codes the triggers in a 32 bits string giving all the pointing tracks with a position resolution of 8cm.

The trigger data are transmitted synchronously to the Muon Regional Trigger using two optical links for each TS.

3- DTBX CHAMBER TRIGGER DESCRIPTION

3.1 - Bunch and Track Identifier

The Bunch and Track Identifier has been studied aiming to the identification of the tracks giving a signal in at least three planes of a SL and therefore to reject all uncorrelated single hits. Everytime at least three hits are aligned, a trigger candidate track is detected and the BTI generates a trigger signal with track impact parameters and one quality bit.

The parameters, defined in Fig. 4, are the angle ψ , measured nominally with a resolution better than 60mrad, and the position, given in the SL central plane with a resolution of 1.25mm, both in 6 bit words.

The angle is given implicitly by the angular k-parameter $k = h \tan \psi$ where h is the distance between the wire planes and ψ is the angle of the track projected in ϕ or θ view with respect to the normal to the chamber plane in the same view.

Each BTI is connected to nine wires allocated as shown in Fig. 4. The BTI trigger requires that the hits belonging to the track are aligned within the BTI position sensitivity and that the track k-parameter is within the programmed angular acceptance. With the present geometric parameters of the chamber the angular acceptance is $\psi_{MAX} = \pm 57^\circ$. In the θ view there is no bending due to magnetic field, hence the acceptance can be set for each BTI to trigger on tracks pointing to the event vertex, accounting only for the Coulomb multiple scattering and the beam spot size.

The track information is accompanied by a TRG signal and is transmitted with fixed delay equal to T_{MAX} plus 4 clock cycles needed for input signal synchronization and BTI calculations.

Each chamber SL is equipped with one BTI every four wires and then the BTIs are overlapped by five wires assuring that every track, with angle within the maximum acceptance

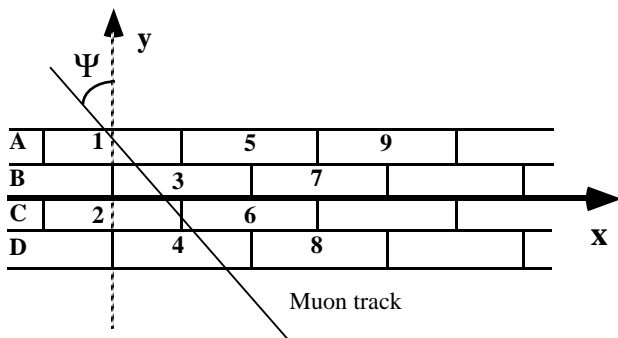


Fig. 4: Chamber section in the bending plane and BTI allocation.

range, is fully contained in at least one BTI. No redundancies are generated because the BTI internal track selection allows every track to be recognized only by one BTI.

The BTI track candidate finding algorithm starts from several track patterns hypothesis: a pattern is identified from a sequence of wire numbers and labels stating if the track crossed the tube to the right or the left of the given wire (e.g. in Fig. 4 the track corresponds to the pattern 1R3L6L4R). For any given pattern the position (*x-equation*) and the k-parameter (*k-equation*) measured by each one of the six couples of planes (AB, BC, CD, AC, BD, AD) can be computed.

In the first step of the BTI logic all *k-equations*, measuring the track k-parameter, are calculated. Then all track patterns are checked and a BTI trigger is generated if at least three of the six associated k-parameters are in coincidence. This coincidence allows the bunch crossing identification owing to the time-dependence of the equations value. The coincidence tolerance of the *k-equations* is defined according to the resolution of each couple that depends on the distance between them. The tolerances on the alignment of hits were chosen to allow a maximum cell linearity error corresponding to 25ns.

If there is a coincidence of six out of six k-parameters, the trigger corresponds to the alignment of four hits and is marked as High Quality Trigger (HTRG), while in any other case it is due to the alignment of only three hits, giving at least three coincident k-parameters out of six, and is marked Low Quality Trigger (LTRG). The angular resolution of LTRGs is track pattern dependent and is generally worse than the one of HTRGs.

If several track patterns give a good response, the HTRG is chosen as the triggering track pattern. If there is more than one HTRG or the triggers are all LTRGs, the first one, in an arbitrarily defined order, is selected. K-parameter and position of the track as measured from the corresponding equations, coded in 6 bits, and one trigger quality bit, marking HTRG or LTRG (H/Lb), are transmitted on the BTI track_data bus.

3.2 - Simulations of the BTI Circuit

The BTI circuit was carefully simulated, assuming a single-hit front-end electronics, using both a functional model, written in FORTRAN, and a VERILOG model, obtaining the same results.

A deep understanding of the BTI performance cannot be obtained from a global simulation, since too many factors contribute to the overall efficiency. We have therefore decoupled the most important effects.

3.2.1 - Influence of Geometrical Inefficiencies and Soft δ -rays Production

The largest background seen with the RD5 studies was the production of *soft δ -rays* [4]: although peaking close to the muon position their production probability at a distance

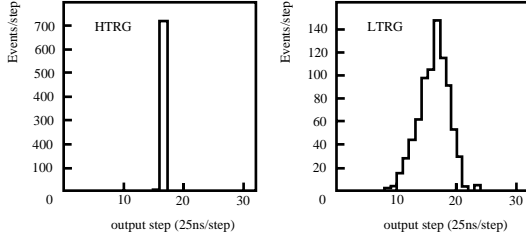


Fig. 5: BTI trigger spectrum with "soft δ rays" background for 867 generated events.

greater than 4σ of the chamber resolution was measured to be $\sim 5\%$ per cell independently of the muon momentum.

The propagation of the signal along the wire and a time resolution $\sigma = 4\text{ns}$ were applied to drift times. Muon secondaries were only *soft δ -rays* (i.e. fully contained in a cell) with a probability of 5%/tube with the spatial distribution parameterized from RD5 data. The electromagnetic showers were not generated. The drift velocity was constant ($V_d = 50\mu\text{m/ns}$) and uniform in the cells. Of course other hits alignments are identified at the wrong bunch crossing. In Fig. 5 we see the full time spectrum in steps of 25ns of the trigger output separately for HTRG and LTRG signals.

In the case of a HTRG in coincidence with a LTRG the first one is always selected. There are LTRGs at the correct step coming from events where one of the muon hits was masked from an electron hit closer to the wire, but there are also LTRGs at the wrong step due to *ghost tracks*: since the BTI is processing in parallel all the possible patterns at each step, some false alignments of three hits of any pattern may happen, due to the unsolved left-right ambiguity. A careful BTI acceptance tuning helps in reducing the trigger noise associated to background particles and to *ghost tracks*, but essentially at least one LTRG at some wrong step is associated to each HTRG at the correct step.

One way to get rid of this problem is the *Low Trigger Suppression (LTS)* algorithm: LTRGs are suppressed when they are within $\pm n$ bunch crossings from a HTRG. With this algorithm it is necessary to add a latency of other n cycles.

The results of the simulation showed that the probability of having a trigger signal at the correct bunch crossing (eff bx) is 97.4%, while the fraction of times where the track candidate at the correct step had the simulated muon actual direction (eff k) within $\pm 120\text{mrad}$ is 94.2%.

While the probability of a HTRG to be wrong is very low, the probability that a LTRG is out of time is high. Infact while the *ghost LTRGs* generated at the wrong step associated to a HTRG are cancelled by the LTS algorithm, they cannot be suppressed when only a LTRG signal can be generated at the correct step, due to the geometrical inefficiencies or the spoiling effect of the background electrons. Unfortunately in this case the probability of wrong noisy signals is about 100%.

3.2.2 - Influence of Drift Velocity Variations

In the same simulation conditions the sensitivity to the drift velocity has been studied (Fig. 6): drift velocity was changed in the range of ± 25 ns around the nominal T_{max} . The BTI can

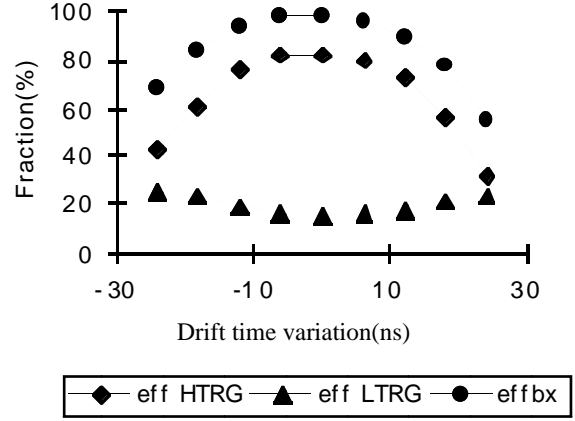


Fig. 6: BTI efficiency versus maximum drift time change.

be programmed for any drift velocity, but the programmability step corresponds to 12.5ns of maximum drift time change.

The DTBX chambers are inserted in the gaps of the CMS magnet return yoke. Therefore the chamber borders near iron discontinuities are affected by a magnetic stray field. The effect is an elongation of the drift time, at least for low field values not distorting too much the electron drift lines. Therefore a simple calculation of magnetic field effects on BTI efficiency can be performed using the previous results.

Two different gas mixtures (Ar:CO₂ 80:20 and 85:15) were considered; the electric field in the cell was assumed constant and high enough to assure the saturation of drift velocity.

The BTI efficiency loss, interpolated from the calculated values is plotted in Fig. 7. The loss can be reduced programming the BTI for an average effective drift velocity.

3.2.3- Summary of BTI Simulations

Simulations evidenced that the main problems affecting BTI performance are the *ghost tracks* and the effects of magnetic field and drift velocity variations. For the latter the BTI programmability allows to change the nominal value of

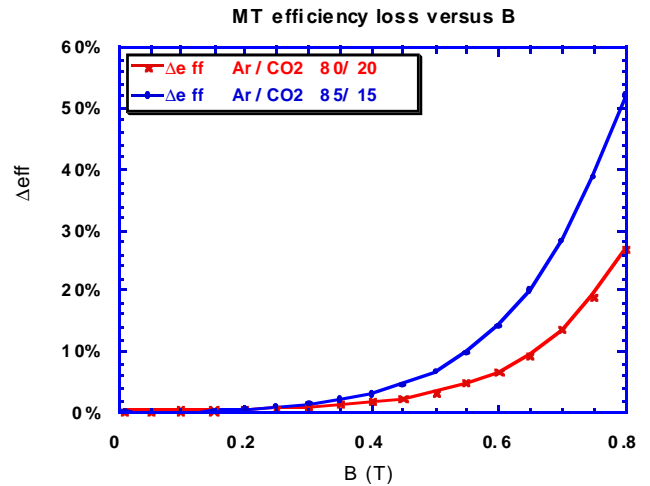


Fig. 7: BTI efficiency loss versus B.

the maximum drift time in 12.5ns steps, while for the former the adopted solution of the LTS algorithm is not fully satisfactory, due to the added latency and the impossibility of acting in absence of any HTRG signal.

In the bending plane there is another possible way to filter *ghost tracks* trying a correlation between the two SLs of the φ view: the simulation results will be given in the Track Correlator paragraph. Anyway, since such a possibility is not available in the θ view, the LTS algorithm is the only way to reduce the LTRG noise in the non-bending projection.

Furthermore the drift cell has been parameterized from GARFIELD [5] calculations, to remove the approximation of a uniform drift velocity inside the tube, and simulated with full background (i.e. including electromagnetic showers too) and without the LTS algorithm.

The BTI efficiency versus muon transverse momentum of these final simulation conditions is summarized in Fig. 8. The effect of muon showering causes a dependence on momentum of the inefficiency, while the small differences between the two SLs are due to the opening of the shower.

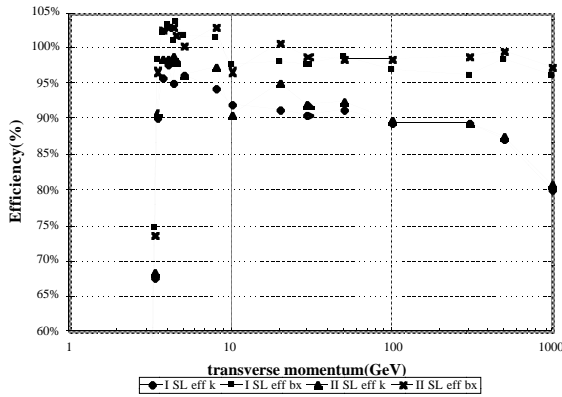


Fig. 8: BTI efficiency versus muon transverse momentum.

3.3 - Track Correlator

A device called Track Correlator has been studied aiming to reduce the BTI noise to an acceptable level and to fix the amount of trigger data in order to satisfy the general requirement that trigger electronics is synchronous and dead time free.

The correlation mechanism of the TC is shown in Fig. 9. The correlation is performed comparing the angles of the two trigger candidate tracks in the outer SL and in the inner SL (ψ_O and ψ_I) and the angle computed using the two positions x_O and x_I (ψ_{COR}). If these three angles are equal, within a programmed tolerance, the track candidates are flagged as correlated. In this case only the correlated track data packet is transmitted to the next trigger stage.

The resolution of ψ_{COR} is 10mrad and the position of the correlated track is given on the chamber x-axis.

In the case of uncorrelated track segment(s), the trigger quality bit H/Lb is used to decide which track candidates will be forwarded to TS φ . The BTI simulations showed that HTRGs are almost always at the correct time and they can be safely transmitted without any filtering; it is instead important

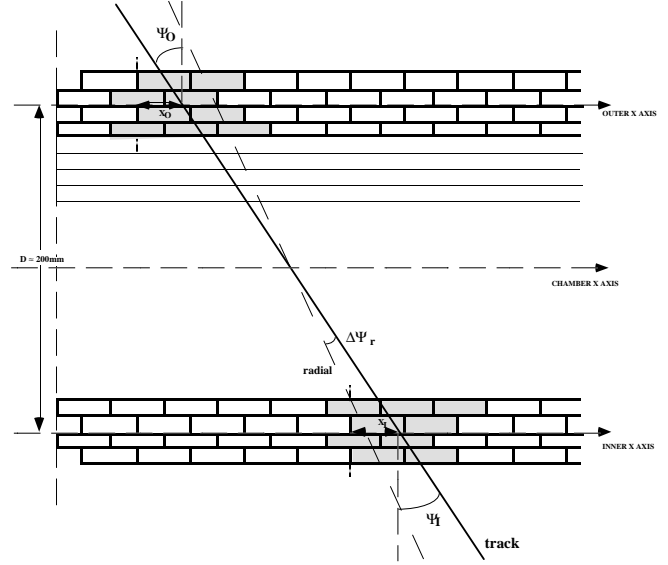


Fig. 9: Explanation of the correlation mechanism.

that single LTRGs are filtered because *ghost tracks* belong to this class. A simple way to filter them is to look for a time coincidence with the trigger coming from the SL of the θ view, on which a sizeable ghost reduction is already obtained from its much lower angular acceptance and, if necessary, a larger one can be obtained applying the LTS algorithm.

The proposed TC structure is shown in Fig. 10: each TC is connected to five BTIs of the inner SL and fifteen BTIs of the outer one. The overlap between TCs is only in the outer BTIs and does not create redundancies, since the BTIs of the outer SL have a dedicated output port for every TC connected to them, filtering only tracks pointing to the inner BTIs of the TC.

Triggering tracks are evaluated, selecting only the two tracks with the angles closest to the radial direction ψ_r , and transmitted to the next trigger stage.

BTI candidates for correlation are selected in each SL twice in pipeline, searching for the lowest $\Delta\psi_r$. If the choice of the track segments is done ignoring the H/Lb it may happen that both track segments are *ghosts*. In order to be sure that at least one track is a real one, it has been decided that HTRGs are preferred for the first track selection, while for the second selection all remaining BTI triggers are considered.

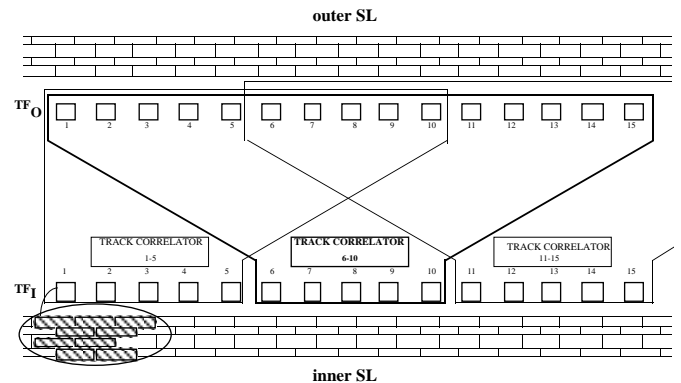


Fig. 10: Track Correlator allocation.

If the correlation was not successful only one uncorrelated track segment is transmitted. If the track segments are of the same quality, the track in the inner SL is preferred because it is not redundant.

The computed track parameters are given with a latency of 5 bx as: 8 bits for the angle (k), 8 bits for the position (along the chamber center axis) with a resolution of 2.5mm and some bits qualifying the trigger as required by the Muon Regional Trigger specifications.

3.4 - Trigger Server

The main function of the $TS\phi$ device is to select among all the candidates transmitted by the chamber TCs two tracks choosing the track angles closest to the radial direction, and to transmit them to the Muon Regional Trigger. Receiving in advance from all connected TCs in parallel the $\Delta\psi_T$ value in 5 bits the reading sequence can be prepared using a common data bus and one enable line for each TC.

Track selection is performed in two clock cycles in pipeline with TCs operations: in the first step the lowest radial angle difference is selected among all the first track candidates elaborated by TCs; in the second step the same is done with the list of second track TC candidates.

The two tracks are transmitted in one clock cycle using optical links. The track parameters are: the angle in 8 bits with a resolution of 10mrad (effective only for correlated tracks: 60mrad otherwise), the position in 11 bits with a resolution of 2.5mm converted in chamber coordinates and some bits as trigger qualification informations.

The TS of the non-bending projection performs the wired-or of the TRG outputs of all the BTIs of the θ view and sends it to the TCs of the ϕ view; in addition all the TRGs are coded in 32 bits giving the position of all the detected tracks with a resolution of 8cm.

As already mentioned, due to the high noise level related to *ghost tracks*, the LTS algorithm is necessary and the best compromise between latency and trigger noise is the suppression of the LTRGs of one bunch crossing before and 8 bunch crossings after a HTRG.

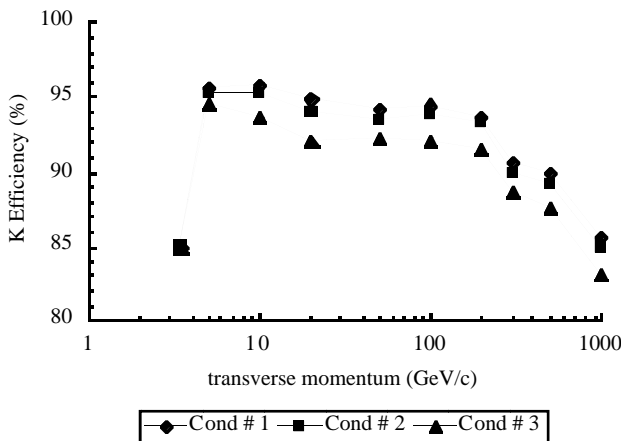


Fig. 11: ϕ view efficiencies at Station 1 for some θ coincidences.

3.6 - Simulation of the Correlator/Server Chain

The complete trigger chain was simulated in FORTRAN using the CMS Technical Proposal layout of the detector.

The parameters that were supposed to be programmable in the chamber trigger logic were: the application of the LTS algorithm, the tolerance for the correlation in the ϕ view ($\Delta k\phi_{COR}$), the acceptance for the BTI of the θ view ($\Delta k\theta$) and the kind of correlation between the trigger in ϕ and θ views. Tolerances and acceptances are set in units of the k -parameter. Efficiencies and noise of the trigger depends on the choice done on these parameters.

The correlation between views happened to be the parameter with the most effective impact on performances. This parameter is only acting on the possibility of passing to the $TS\phi$ and successively to the Muon Regional Trigger the single LTRG candidate tracks of the TCs. Fixing the tolerances $\Delta k\phi_{COR} = 2$ and $\Delta k\theta = 1$ the efficiencies as function of muon transverse momentum for tracks generated with $-1 < \eta < 1$ in the full ϕ range are given for the following conditions in station 1:

Cond. # 1 Single LTRG accepted only if there was any TRG in $TS\theta$

Cond. # 2 Single LTRG accepted only if there was an HTRG in $TS\theta$

Cond. # 3 Single LTRG not accepted

The results are normalized to a reference sample of tracks in order to subtract the contribution of geometrical inefficiencies and border effects and get the actual trigger chain efficiency.

From the graphs of Fig. 11 it can be noted that there is a sharp cut at low momentum due to the ranging out of the muons and a loss at high momentum due to the destructive effect of the electromagnetic showers generated from the muon interaction with matter.

The fraction of correctly identified muons falling in the different correlation categories is plotted in Fig. 12. As an effect of the muon showering the fraction of correlated tracks is slowly decreasing with momentum.

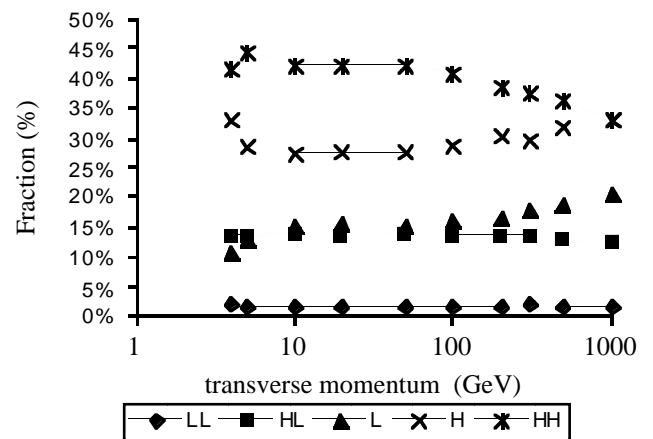


Fig. 12: Code fractions for $TS\phi$ candidate tracks.

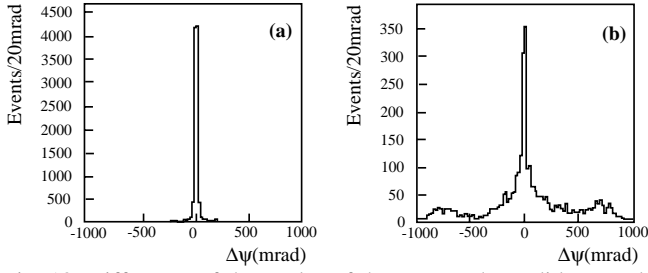


Fig. 13: Difference of the angles of the BTI track candidates and of the generated muon at the muon chamber entry for (a) triggers at correct bx and (b) triggers at wrong bx.

As an example in Fig. 13 we show the difference between the direction measured by the BTI and the actual muon angle at entry of the chamber for $p_T = 100\text{GeV}/c$. The plots are shown for the sample of candidates triggering at the right bunch crossing and the ones triggering at the wrong one.

4 - HINTS ON THE PERFORMANCE OF THE DTBX MUON REGIONAL TRIGGER

The Trigger Server sends the information to the DTBX Muon Regional Trigger [6], that is supposed to link the track candidates in the different chambers to forward to the Global Trigger a clean muon candidate.

A rough estimation of the efficiency of this step of the trigger system can be obtained looking at the coincidence of the track candidates in different chambers.

In the following analysis a muon was supposed to be correctly identified in a station if the difference between the angle of the track candidate and the actual muon angle at station entry was less than 120mrad . No check was done on the muon position. We have looked to two kinds of time coincidences, in the four stations of the barrel system, of the candidates correctly identified in n out of four ($n/4$) stations:

- (2/4) $_{\phi}$ two out of four candidates in coincidence in ϕ view
- (3/4) $_{\phi}$ three out of four candidates in coincidence in ϕ view.

The efficiencies of the Muon Regional Trigger, assuming a perfect performance of its track finding algorithm, for these categories of coincidence is plotted in Fig. 14.

The execution flow chosen for the TC logic was the first one of paragraph 3.6 (i.e. single LTRG in ϕ view were accepted only if there was any TRG θ , the tolerances were

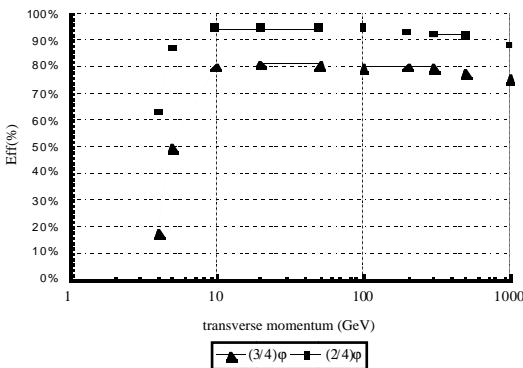


Fig. 14: Muon Regional Trigger efficiency for Cond # 1.

$\Delta k\phi_{\text{COR}} = 2$ and $\Delta k\theta = 1$).

It should be noted that the simulated range extends to $\eta = \pm 1$, therefore there is a non negligible effect due to the absence of contribution of the muon forward chamber from the trigger, especially for the (3/4) $_{\phi}$ coincidence.

A relevant effect of the Muon Regional Trigger is the reduction of the *ghost tracks* background satisfying the correlator filtering logic. In Fig. 15 the trigger output time spectra for $100\text{GeV}/c$ p_T muons are plotted, allowing a comparison between the logic OR of the station trigger outputs and a trigger based upon a coincidence of two out of four or three out of four stations. The relative noise levels for the ϕ view, calculated as percentage of out of time triggers goes from 33.6% for the single station trigger, to 15.8% for the 2/4 coincidence and 2.3% for the 3/4 coincidence.

A similar calculation for the θ view gives approximately the same results.

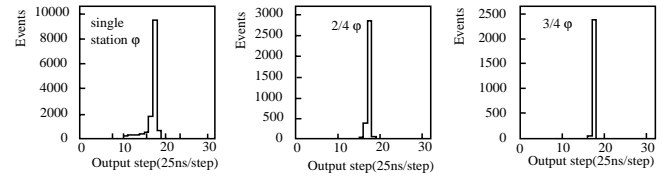


Fig. 15: Effect on the noise in ϕ view for several trigger types.

5 - CONCLUSIONS

The presented trigger structure is still under development, trying to match as well as possible the requirements of the barrel muon trigger and to identify the instruments needed to setup the trigger chain *on the field*.

The trigger system acceptance allows to identify muons in a large momentum range, starting to lose efficiency around $5\text{GeV}/c$ transverse momentum due essentially to muon ranging out. The loss at higher momenta is due to the effect of muon showering.

Several possibilities allowed from the programmable logic have a large impact on noise and efficiency. In particular changing the kind of correlation between the ϕ and the θ views or selecting different track correlation acceptances in the TCs allows to balance between efficiency and noise of the chamber trigger.

REFERENCES

- [1] CMS Technical proposal, CERN LHCC 94-38, LHCC/P1 (1994).
- [2] F. Gasparini et al., Nucl. Instr. and Meth. A336(1993)91-97.
F. Gasparini et al., Nucl. Instr. and Meth. A344(1994)137-142.
G. Barichello et al., Nucl. Instr. and Meth. A360(1995)507-511.
- [3] M. Della Negra et al., CERN/DRDC/90-36, DRDC/P7 (1990).
- [4] C. Albajar et al., "Electromagnetic Secondaries in the Detection of High Energy Muons", CERN PPE/94-204, Submitted to Nucl. Instr. and Meth.
- [5] R. Veenhof, GARFIELD manual, CERN/POOL W5050 (1994).
- [6] A. Kluge, These Proceedings.